

# High spatial resolution analysis of fungal cell biochemistry – bridging the analytical gap using synchrotron FTIR spectromicroscopy

Susan Kaminskyj<sup>1</sup>, Konstantin Jilkin<sup>2</sup>, Adriana Szeghalmi<sup>2</sup> & Kathleen Gough<sup>2</sup>

<sup>1</sup>Department of Biology, University of Saskatchewan, Saskatoon, SK, Canada; and <sup>2</sup>Department of Chemistry, University of Manitoba, Winnipeg, MB, Canada

**Correspondence:** Susan Kaminskyj,  
Department of Biology, University of  
Saskatchewan, Saskatoon, SK, Canada. Tel.:  
+1 306 966 4422; fax: +1 306 966 4461;  
e-mail: susan.kaminskyj@usask.ca

**Present address:** Adriana Szeghalmi,  
Max-Planck-Institut für Mikrostrukturphysik,  
Weinberg 2, D-06120 Halle, Germany.

Received 14 December 2007; accepted 7 March  
2008.

DOI:10.1111/j.1574-6968.2008.01162.x

Editor: Richard Staples

## Keywords

infrared spectroscopy; filamentous fungi; high  
spatial resolution; biochemical composition;  
single cell.

## Introduction

Fungi have diverse impacts on the environment and on human affairs, both positive and negative. These range from nutrient recycling, formation of mycorrhizae and important roles in biotechnology, to being established or emerging animal and plant pathogens. Some fungi can be benign or dangerous depending on the circumstance, for example, *Aspergillus fumigatus* is a saprotroph, but it can also be an opportunistic human pathogen (Firon & d'Enfert, 2002). Both biology and environmental context can influence the outcome of fungal growth. Despite their obvious morphological differences, fungi and animals share important physiological similarities (Baldauf *et al.*, 2000), and so a better understanding of fungal metabolism has broad relevance to humans.

Cell composition, structure and function are interrelated. Cells contain genetic material (DNA and RNA), gene

## Abstract

Fungi impact humans and the environment in many ways, for good and ill. Some fungi support the growth of terrestrial plants or are used in biotechnology, and yet others are established or emerging pathogens. In some cases, the same organism may play different roles depending on the context or the circumstance. A better understanding of the relationship between fungal biochemical composition as related to the fungal growth environment is essential if we are to support or control their activities. Synchrotron FTIR (sFTIR) spectromicroscopy of fungal hyphae is a major new tool for exploring cell composition at a high spatial resolution. Brilliant synchrotron light is essential for this analysis due to the small size of fungal hyphae. sFTIR biochemical characterization of subcellular variation in hyphal composition will allow detailed exploration of fungal responses to experimental treatments and to environmental factors.

products (proteins) and products of gene products (carbohydrates and lipids), often in combination (e.g. glycoproteins). Fungi are exemplary models for studying eukaryote biology because their simple shapes and growth habits facilitate analyses, while the underpinnings of their metabolism can be explored using molecular and genetic tools. There are clear relationships between fungal morphogenesis and metabolism. For example, citrate secretion by industrial strains of *Aspergillus niger* uses growth conditions that perturb hyphal morphology (Karaffa & Kubicek, 2003).

Cell polarity, that is, the ability to maintain regions of cytoplasmic specialization, underpins growth and differentiation in living organisms. Fungal growth is spatially constrained to cell tips, which can generate tubular hyphae as well as individual yeast cells (Bartnicki-Garcia, 2002). In general, hyphal tips grow continuously, given sufficient nutrients and space. Their relatively quiescent basal regions can form new tips in order to branch, or can differentiate for

asexual spore development. Many fungal genomes have been sequenced, and a wealth of experimental tools has been developed to explore this resource. Improved analytical methods for high spatial resolution studies of fungal cell biochemical composition will allow for more precise documentation of the phenotypic consequences of genetic manipulations that can be related to cell structure and function. This review will focus on the principles and application of synchrotron Fourier transform infrared (sFTIR) spectromicroscopy that can profile major component types and abundances.

### Current methods for exploring cell composition – strengths and limitations

Cell polarity is intrinsic to fungal growth. The tremendous variations in cytoplasm structure and function between tip and subapical regions, reviewed in Bartnicki-Garcia (2002), imply related differences in cell composition. In general, the number and types of component that can be studied simultaneously are inversely related to the spatial resolution of the analysis method. For example, the identities of hundreds of components can be resolved in bulk samples using gas chromatography-MS, whereas the distribution and behavior of one or a few components can be assessed at a much higher resolution using histochemistry or fluorescent tagging. Detailed ultrastructural studies of fungi show that their morphology and hence composition is likely to change dramatically over many microns. At least two methods can (or have shown promise to) span this technique-related gap and to have exceptional analytical power: single-cell sFTIR spectromicroscopy (discussed below) and Raman microscopy (Szeghalmi *et al.*, 2007b). Both techniques provide a rich biochemical signature arising from pixel sizes on the order of a few microns. Other methods are reviewed in Navratil *et al.* (2006) and Kaminskyj & Dahms (2007).

Classical and molecular genetics have shown that genes often function in pathways (Beadle & Tatum, 1941), and that each gene product can have multiple interactions (e.g. [www.yeastgenome.org/GOContents.shtml](http://www.yeastgenome.org/GOContents.shtml)). Genomic profiling can relate metabolic state to gene transcription activity, but relative transcript abundance does not necessarily relate directly to transcript persistence, translation rate, post-translational modification or translated product stability. As a result, genomic profiling can address some effects of genetic and environmental manipulations but cannot directly assess changes in cell composition.

As a complementary method, biochemical profiles of carbohydrates, proteins, lipids and nucleic acids can be generated with FTIR spectromicroscopy, with spatial resolution at the diffraction limit of the infrared spectrum, as low as 3  $\mu\text{m}$  at the shorter wavelengths (Szeghalmi *et al.*, 2007a;

Jilkine *et al.*, 2008). FTIR analysis of fungal cells is challenging because much of the relevant information on cell walls and energy sources resides in the carbohydrate composition, but the most distinctive carbohydrate signatures are at the longer infrared wavelengths (c. 10  $\mu\text{m}$ ) where the diffraction limit and scattering artifacts restrict spatial resolution and signal strength. The amount of material in fungal hyphae and spores is small but, with a bright synchrotron source to offset these issues, sFTIR can be used to probe subtle and cell type-specific biochemical differences in fungal systems. A key feature of sFTIR spectromicroscopy is the capability for multiple component identification and localization in pristine tissue. Preparation is minimal; relative amounts and structure of tissue constituents can be ascertained *in situ*; nothing is lost through solvent extraction; and likewise, nothing is added or perturbed by fixation or staining.

### A primer on FTIR spectromicroscopy of biological materials

Briefly, infrared spectroscopy refers to the measurement and analysis of the wavelengths of infrared light preferentially absorbed by a specimen (Wilson *et al.*, 1955). A unique set of specific infrared energies will be taken up by each molecule, determined by the types of molecular vibrational motion excited (for example, bond stretch and interbond angle change), the types of chemical bonding and the masses of the atoms involved. Unlike visible light microscopy, FTIR spectroscopy reports energies of absorbance peaks in wavenumbers ( $\text{cm}^{-1}$ , inverse wavelength). Typical vibrational energies lie in the mid-infrared region, 4000–800  $\text{cm}^{-1}$ , corresponding to wavelengths between 2.5 and 12.5  $\mu\text{m}$ . The data are displayed as absorbance peaks ( $y$ -axis) as a function of infrared energies (wavenumbers,  $x$ -axis), constituting the infrared spectrum.

Infrared spectroscopy of biological materials was first investigated in the early and mid 1900s (Coblentz, 1911; Darmon & Sutherland, 1947; Blout & Fields, 1948; Blout & Mellors, 1949; Elliott & Ambrose, 1950), including the first spectroscopic experiments on microtomed tissue sections (Blout & Mellors, 1949; Fraser, 1950). Widespread use in the biological sciences began with the advent of the interferometer-based instruments (FT-IR) in the 1970s (Becker & Farrar, 1972; reviewed in Naumann, 1985). Since then, FTIR has become a recognized tool for the analysis of model systems *in vitro* as well as of components in tissues *in situ*. Today, there are many outstanding references for instrumentation, applications and guidelines to spectral interpretation (Griffiths, 1975; Griffiths & De Haseth, 1986; Messerschmidt & Harthcock, 1988; Chalmers & Griffiths, 2002; Everall *et al.*, 2007).

In recent years, FTIR spectromicroscopy, that is, high spatial resolution FTIR, has been used for studying cell

composition stages of mitosis (Jamin *et al.*, 1998), apoptosis (Holman *et al.*, 2003) and regulation of homeostasis (Montechiaro *et al.*, 2006). These studies show that the low power of the synchrotron source causes only minimal sample heating ( $< 0.5\text{ }^{\circ}\text{C}$ ) and so, unlike X-ray spectroscopy, no sample damage is incurred. Bulk infrared analyses of fungal masses have been used to differentiate *Candida* species (Toubas *et al.*, 2007). We have demonstrated the potential for sFTIR imaging and spatially resolved biochemical analyses of fungi (Szeghalmi *et al.*, 2007a; Jilkine *et al.*, 2008).

The typical instrument consists of a light source (either a hot ceramic globar or a synchrotron beam), an interferometer, a microscope with sample stage and a detector interfaced to a computer for data collection and analysis. Visible light is used to define the region of interest, followed by infrared light for spectromicroscopy. A motorized platform enables raster scanning across the sample (mapping). Instruments equipped with a focal plane array (FPA) detector can collect many spectra simultaneously from a large area. A wide range of spectral data processing options are available to illustrate the distribution and relative concentration of different tissue components (Gough *et al.*, 2005). For sFTIR using the reflection mode, the specimen is mounted or is grown on an infrared-reflective substrate; both illumination and detection are from above. In this case, the intensity of a given absorbance peak is proportional to  $\log 1/R$ , where  $R$  is the ratio of light reflected by the sample to that reflected by the bare substrate.

Relevant factors for the success of FTIR analysis are spectral resolution and spatial resolution. The first refers to the difference in the absorbance energies for targets of interest (functional groups, significant conformational differences); a significant energy separation between strong absorbances in the spectrum is ideal but not essential. The second depends on the physical size and distribution of absorbing fractions and the wavelengths of light at which their characteristic absorptions occur.

### Presence of strong absorbances from different chemical components

Figure 1 illustrates the surprising simplicity of the infrared spectrum of human brain tissue in which strong, energetically resolved protein, lipid, sugar and phosphate bands appear. The  $1800\text{--}800\text{ cm}^{-1}$  region of the infrared spectrum contains many overlapping bands from chemical functional groups, representing the sum of all the vibrational modes of all the groups present. The carbonyl group in lipids absorbs at a higher energy than that in proteins, because lipid  $\text{C}=\text{O}$  is typically not hydrogen bonded to any nearby proton donors. In proteins, the  $\text{C}=\text{O}$  functional groups form hydrogen bonds with neighboring  $\text{N-H}$  groups, weakening the bonds and lowering their vibrational energy; addition-

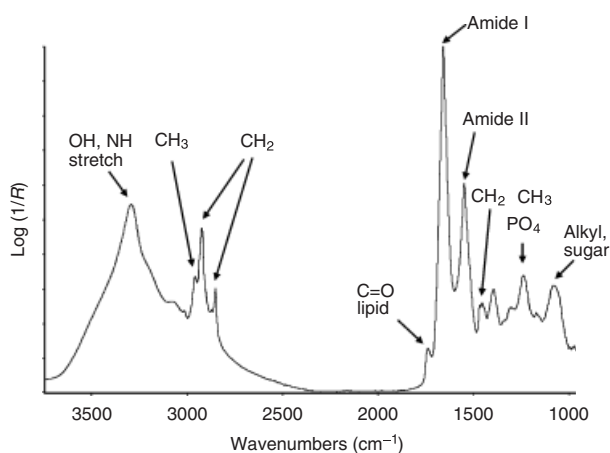


**Fig. 1.** A typical brain tissue spectrum in the mid-infrared (Rak, 2007, with permission) showing the general assignment of peaks to some functional groups found in normal human brain tissue, between  $4000$  and  $800\text{ cm}^{-1}$ . Spectrum recorded at National Synchrotron Light Source,  $4\text{ cm}^{-1}$  spectral resolution,  $15\text{ }\mu\text{m} \times 15\text{ }\mu\text{m}$  aperture, tissue section  $10\text{ }\mu\text{m}$  thick. Brain tissue contains abundant protein and lipid, but relatively little carbohydrate. The higher energy region ( $2600\text{--}3500\text{ cm}^{-1}$ ) exhibits characteristic absorbance peaks due to the stretch of  $\text{N-H}$  and  $\text{O-H}$  bonds. The  $\text{C}=\text{O}$  of fatty acid esters appears at about  $1740\text{ cm}^{-1}$ . In brain tissue, the region from  $1800$  to  $800\text{ cm}^{-1}$  is dominated by protein (Amide I and II), phosphate and sugar bands, along with other small but significant peaks. The absorbance ( $\log 1/R$ ) is proportional to the relative concentration; the absolute concentration of individual components must be determined via separate calibration procedures.

ally, the strength of the interaction varies with the protein secondary structure. Thus, the so-called amide I band that appears between  $1690$  and  $1620\text{ cm}^{-1}$  and the amide II band, due to modes that involve the  $\text{H-N-C}$  angle bend and  $\text{C-N}$  stretch around  $1550\text{ cm}^{-1}$ , are used as a proxy for proteins and their secondary structure. Bands observed at  $1238$  and  $1075\text{ cm}^{-1}$  have been ascribed to phosphate groups in nucleic acids and phospholipids. Sugars, whether mono- or polymeric, exhibit strong bands in the  $1150\text{--}900\text{ cm}^{-1}$  region due to ring  $\text{C-O-C}$  vibrations. The latter are particularly important for fungal sFTIR (Szeghalmi *et al.*, 2007a; Jilkine *et al.*, 2008). The higher energy, shorter wavelength region ( $2700\text{--}3400\text{ cm}^{-1}$ ) contains bands due to  $\text{CH}$ ,  $\text{NH}$  and  $\text{OH}$  stretch modes.

While it is possible to ascribe some peaks to sugars, nucleic acids, proteins and lipids, certain precautions are important. The FTIR spectrum of a pure compound is unlikely to be the same when that compound is within the complex cytoplasm matrix. FTIR results must be validated by stringent comparison with data obtained using other analytical methods. For example, Szeghalmi *et al.* (2007a) compared their FTIR spectra with a wealth of data from light and electron microscopy, and from biochemical and genetic analyses. Furthermore, sFTIR data were collected from individual hyphae at defined distances from the hyphal tip.

In biological samples, it is possible, but not common to identify unambiguously a particular compound in a mixture (e.g. Gallant *et al.*, 2006). It is impossible to distinguish between differences in DNA or RNA base pair sequence, but for the latter we have powerful molecular genetic tools. Nevertheless, sFTIR allows carbohydrate, lipid and protein profiling at a high spatial resolution, and the fact that cellular context can have dramatic effects on peak location can be successfully exploited.

### Separation between the strong absorbances in the spectrum

Spectral resolution refers collectively to intrinsic sample limitations and instrument limitations, some of the latter being operator-controlled. Two bands that naturally occur close together in energy are said to be spectrally resolved if there is a valid detectable minimum between the adjacent band maxima (Rayleigh criterion). One prerequisite is that the interval at which data are being collected must be smaller than the separation between the adjacent bands. However, the absorbance bands of biological molecules are often much broader than the separation between peaks (we typically collect sFTIR data with a wavenumber resolution of  $4\text{ cm}^{-1}$ ), and so many similar bands are closely superimposed. The apparently simple pattern observed in the sFTIR spectrum of sectioned brain tissue (Fig. 1) is the sum of overlapping absorbances at nearly identical wavenumbers and the relative compositional homogeneity of neurons at this spatial resolution. Numerical techniques for artificially enhancing the spectral resolution are sometimes used, and chemometric software tools implementing multivariate statistical spectral analysis methodologies are now standard with infrared microscope instrumentation. Reference libraries describe the typical absorptions of common biological molecules, analyzed as pure compounds. However, as reiterated below, caution must be exercised in interpreting spectra from biological samples.

### Spatial resolution, diffraction limit and choice of detector

Diffraction is an issue because the wavelengths of infrared light impose a physical limit on spatial resolution. For example, at higher energies (wavenumber =  $4000\text{ cm}^{-1}$ ), the wavelength of the light is  $1/\text{wavenumber}$  or  $2.5\text{ }\mu\text{m}$ . Lipids are identified from the  $\text{CH}_2$  stretch vibrations (*c.*  $2850$  and  $2920\text{ cm}^{-1}$ ) with a diffraction limit of about  $3\text{ }\mu\text{m}$ . However, the region of interest for sugars includes ring vibrational modes around  $1000\text{ cm}^{-1}$ , for which the spatial resolution is *c.*  $10\text{ }\mu\text{m}$ . Theoretically, the diffraction limit is roughly  $\lambda/2$ , but the signal to noise ratio can be a problem for individual cells compared with tissue slices, because the amount of material is much smaller. Also, even when the spatial

resolution is on the order of  $3\text{ }\mu\text{m}$ , the *z* dimension of the sample adds to the *xyz* sampling volume.

Where the infrared wavelength matches the dimension of the sample, internal scattering occurs as it passes through the sample, sometimes creating severe baseline distortions (Mie, 1908; Mohlenhoff *et al.*, 2005). Sometimes, this can be mitigated by increasing the aperture slightly. Aperture and mapping step size are controlled independently. If the step size is less than the pixel dimension, pixels will be overlapped (tiled) but this does not affect the quality of each spectrum.

Detector choice is limited by what is available at a particular facility. A single point detector is comparable to a light microscope objective, which collects spectral information from a single pixel. A FPA detector has a linear or two-dimensional array of elements equipped for simultaneous spectral detection from multiple pixels. FPAs are a relatively recent development that is particularly useful for rapidly mapping areas of large samples. While they enable mapping with a bench instrument equipped with a global source, FPAs are nevertheless prone to blurring artifacts (Miller & Smith, 2005). Given that fungal hyphae are flexuous and typically grow relatively widely separated from each other, and that microscopes with mapping capability can be set to acquire spectra from user-defined pixels along a hypha of interest, we concur with Dumas *et al.* (2004) that single-element mapping is likely to be optimal for fungal hyphae. We will be testing an FPA system coupled to a synchrotron source in the near future.

### Value of synchrotron source

Is it possible to study fungal cell composition without synchrotron light? Yes, barely. The production of synchrotron light is beyond this minireview (for a brief overview, see [www.lightsource.ca/education/whatis.php](http://www.lightsource.ca/education/whatis.php)). Most importantly, synchrotron infrared light is about a thousand times brighter than a global, enabling data collection from small samples such as hyphae. As described in Jilkine *et al.* (2008) and Fig. 2, the pixel size for our sFTIR studies was  $10\text{ }\mu\text{m} \times 10\text{ }\mu\text{m}$ , and 256–1024 scans were collected for background and sample sites. From the same specimen, a usable spectrum was collected from a group of spores using the global source in the instrument. In this case, a pixel size of  $35\text{ }\mu\text{m} \times 40\text{ }\mu\text{m}$  and at least 4096 scans were required for background and sample sites. In other words, the synchrotron source improves our data collection rate by a factor of 100–400 times. Practically speaking, it is the only choice for analysis of individual fungal hyphae by FTIR spectromicroscopy.

### Sample preparation for sFTIR spectromicroscopy

A key requirement for informative sFTIR studies is that the specimens must be chemically pristine; chemical fixative or

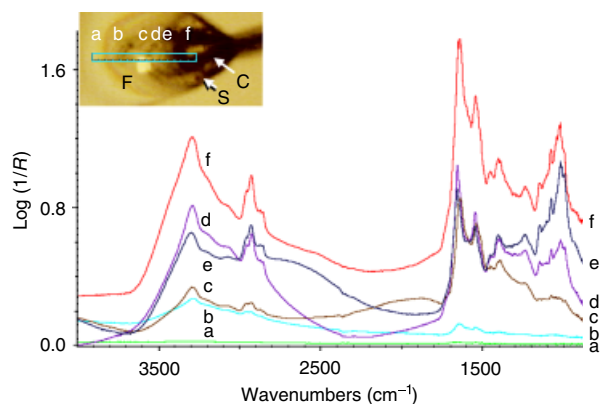


**Fig. 2.** Visible light image (inset) and spectra from a burst *Rhizopus* sporangium that spewed fluid (F) and immature spores (S) onto the FTIR substrate near the columella (C). Spectra (a–f) are representative of the variation across a  $16 \times 2$  map (blue box on the inset), composed of  $10 \mu\text{m} \times 10 \mu\text{m}$  pixels. All spectra have the same baseline. Bands due to lipid, protein, phosphates and sugars are evident; the profiles are distinctly different from those in Fig. 1. Sporangium fluid (spectra a, b, c) has relatively little biochemical content, mostly protein. The increasing intensity (from a to c) reflects the increasing thickness of the dried fluid layer. Immature spores (spectra d–e) contain considerably more biochemical material than the surrounding fluid (overall increase in absorbance intensity) with a particularly significant increase in the sugar and phosphate content, probably indicative of both nuclear and nutrient density. The columella (f), which may be surrounded by additional spores not resolved in the image, has high levels of each type of component. The baseline between 1700 and 2700 wavenumbers is not entirely flat, an artifact typical of thin films and specimens with high topography in regions of low spectral absorbance.

staining procedures are avoided as they would affect the spectra. Scanning electron microscopy typically requires coating with a conductive material (Kaminskyj & Dahms, 2007); however, for specimens that will be used for dual analyses, coating must be deferred until sFTIR is complete. After considerable experimentation, we now prepare filamentous fungi by growing hyphae from inoculated agar media across an infrared-reflective substrate. Substrates include MirrIR slides (available from Kevley Technologies, [www.tientasciences.com](http://www.tientasciences.com)) and gold-coated silicon wafers. The latter can be made relatively economically in a nanotechnology lab, broken into 1-cm squares and fixed to a glass microscope slide with double-sided tape. An advantage of MirrIR is the large surface area and highly reproducible quality; however, Au-coated silicon can be more cost effective for certain experiments. Unexpectedly, *Aspergillus nidulans* grows better on Au, whereas *Neurospora* and certain other species grow better on MirrIR.

Fungal cultures grow out from inoculated agar-solidified media, incubated upright or inverted (supported by glass tubing) in a moist chamber. Fungal hyphae will grow across a nutrient-free substrate, using nutrients that are transported internally. We have noted minor traces of medium transported

by capillary action along the hyphal surface, but typically this is only within a millimeter of the block edge, and the extent is readily apparent using low-magnification light microscopy. Growth should be allowed to proceed for several millimeters from the agar if possible; however, overlong incubation can lead to abnormal growth due to cellular stress.

Spores of some plant pathogenic fungi can germinate under humid conditions on nutrient-free substrates, for example *Magnaporthe grisea* (Howard *et al.*, 1991), but this is not generally the case for saprotrophs. Unexpectedly, although *Aspergillus* and *Neurospora* spore germination is improved considerably in the presence of a fermentable carbon source (d'Enfert, 1997), these spores have been shown to germinate at a low frequency without exogenous nutrients, given a humid environment (Jilkine *et al.*, 2008).

Sample harvest and preservation must be rapid to prevent cell degradation or stress-related changes. Currently, our preferred method is to freeze samples on a  $-80^\circ\text{C}$  metal surface, and then freeze-dry. Fungal hyphae are typically between 2 and  $10 \mu\text{m}$  in cross-section, and because fungal cells are internally supported by turgor pressure, they become relatively flat after being dried onto the FTIR substrate. For species like *Rhizopus* that have upright sporangia, even after inverted incubation, and for those with large hyphae, it can be advantageous to thaw the slide briefly to collapse the cells before freeze drying. An alternative may be to flatten such specimens in an anvil cell; this method is being tested currently. Once dried, the specimens are ready for sFTIR or Raman spectroscopy (Szeghalmi *et al.*, 2007b).

## Data acquisition

Before sFTIR spectrum acquisition, we use a microscope equipped with a  $\times 10$  objective, reflected light and consumer-grade CCD to collect visible light images of the sample in order to identify appropriate regions for analysis, and to make low-magnification 'maps' of cultures (e.g. Fig. 3a and b). This facilitates multiple analyses on the same cell at different facilities or by other techniques. A background spectrum is collected from a clean area on the substrate. Water and  $\text{CO}_2$  have strong infrared absorbances in the  $4000\text{--}800 \text{ cm}^{-1}$  region. sFTIR microscopes are typically jacketed and purged with dry  $\text{N}_2$  to minimize their presence. Additional spectra collected on blank areas before and after mapping are useful if it proves necessary to subtract residual water and  $\text{CO}_2$  peaks.

The variation in cell composition makes it critically important to collect many representative spectra from defined sites in independent samples. Both Szeghalmi *et al.* (2007a) and Jilkine *et al.* (2008) showed using sFTIR that hyphal composition varied with distance from the tip, and with small changes in growth condition. In addition to selecting data free from serious technical artifacts (e.g.

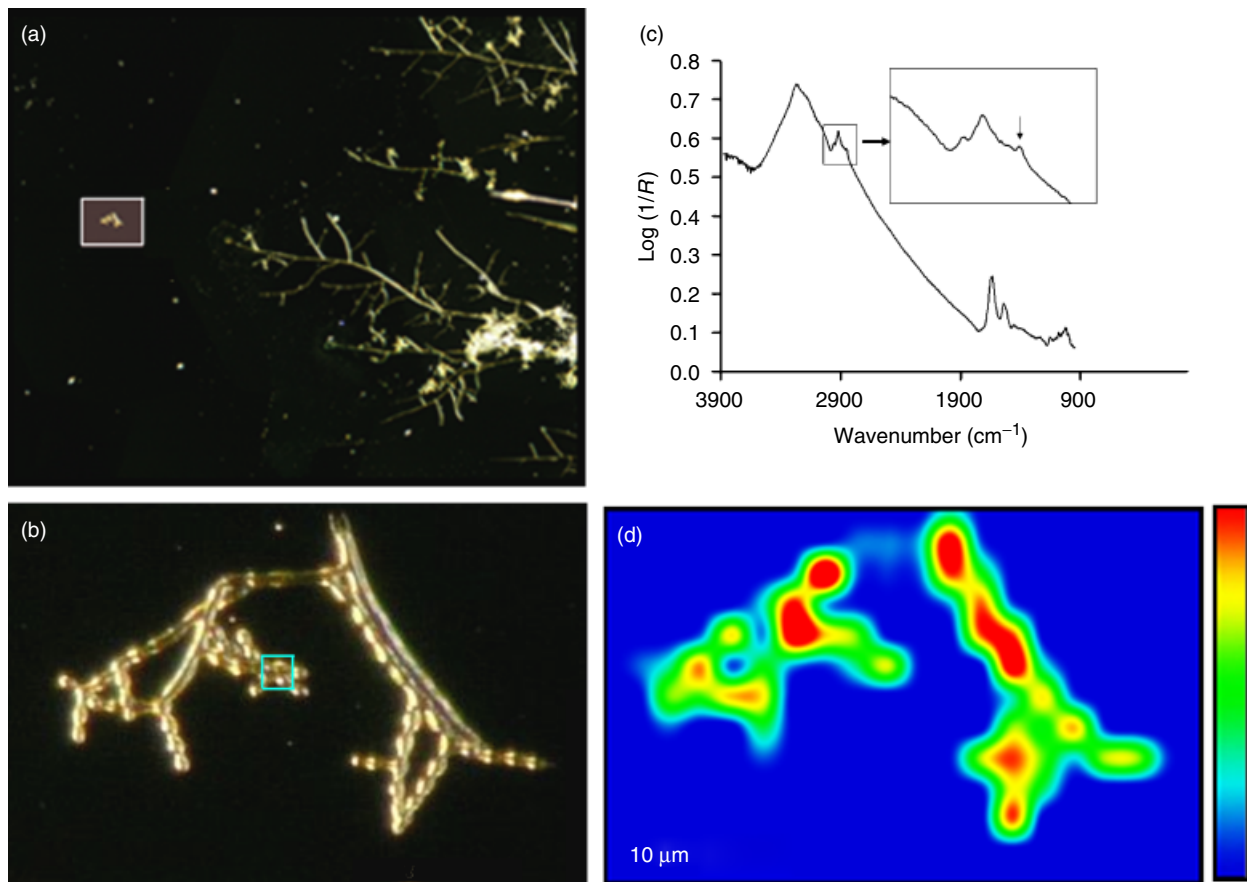


**Fig. 3.** *Neurospora* sporulation. (a) Specimen map image acquired with a  $\times 10$  objective and reflected light. The boxed region indicates a fragment of a sporulating hypha that broke off from the colony and landed nearby, analyzed as shown in b–d. (b) Specimen image acquired with visible light and the  $\times 36$  infrared objective, before collecting FTIR spectra. (c) sFTIR spectrum collected from the blue pixel in (b). The steeply sloping baseline is likely due to Mie scattering. The inset shows expansion of the CH stretch region. (d) A blended spectral map of the spore branch in (b), using the CH<sub>2</sub> peak indicated in (c), likely indicating the presence of lipid or membranes within the spores. High intensity is shown as red.

Fig. 3c), our analyses are based on sFTIR spectra from hyphae with a high biochemical content for their age, site and growth condition. Apart from co-addition of multiple spectra and subtraction of background water absorbance, we use no data smoothing or analysis algorithms, which might introduce interpretational artifacts (Gough *et al.*, 2005; Szeghalmi *et al.*, 2007a; Jilkinė *et al.*, 2008). Spectral interpretation is based on a broad range of sources, as described above. Spectral data can be shown for individual pixels (Figs 1 and 2), or the distribution of a particular absorbance intensity (e.g. Fig. 3c) can be displayed as a pixilated (not shown) or a blended (Fig. 3d) map.

### What has sFTIR spectromicroscopy revealed about fungal cells?

Szeghalmi *et al.* (2007a) and Jilkinė *et al.* (2008) showed that fungal hyphae undergo consistent changes during maturation.

The tips of established hyphae, as well as germ tubes (Jilkinė *et al.*, 2008), contain little biochemical material compared with basal regions. What little there is absorbs most strongly in the amide I and II regions, indicating protein content with lesser amounts of lipid and sugars.

Fungi hyphal composition changes in response to their environment, before morphological changes are evident. *Neurospora* and *Rhizopus* hyphae grown on medium at pH 8.5 were less robust than those grown at pH 6.5; the patterns of stress response differed subtly between the two. *Aspergillus* and *Neurospora* hyphae were dominated by protein, with minor sugar and lipid content, in contrast to *Rhizopus*, which had a considerably stronger, well-defined carbohydrate structure. Jilkinė *et al.* (2008) showed that *Neurospora* spore composition varied relatively little with growth medium pH, suggesting that hyphae might preferentially translocate nutrients to spores at the expense of the vegetative cell. This was supported by spore ontogeny studies in the

same paper. Furthermore, germinated *Neurospora* spores retained a (reduced) nutrient dowry, even after the germ tube was *c.* 100 µm long, consistent with future production of secondary germ tubes. Similarly, current studies of plant endophyte strains (Márquez *et al.*, 2007) have shown that their nutrient use and partitioning is substantially different from saprotrophs like *A. nidulans*.

## Using sFTIR to explore fungal biology

Many filamentous fungal genome sequences have been completed, and gene annotation is ongoing. Plans are underway in some fungal systems for genome-wide gene deletion and gene tagging initiatives that will provide elegant ways to explore gene function. sFTIR will be a useful complementary tool for studying the biochemical consequences of molecular genetic manipulation. For example, sFTIR has already clarified aspects of the *A. nidulans hypA1* restrictive phenotype, showing that the apparent abundance of internal cell membranes shown by transmission electron microscopy (Kaminskyj & Boire, 2004) was not mirrored by an increased sFTIR lipid content (Szeghalmi *et al.*, 2007a). By itself, this finding is of little consequence, but assuming that filamentous fungi are similar to *Saccharomyces cerevisiae*, where about a third of gene knockouts in have 'no phenotype', sFTIR could provide invaluable clues as to the function of unknown gene products.

## Acknowledgements

We are pleased to acknowledge Natural Science and Engineering Research Council (NSERC) Discovery Grant awards to KMG and SGWK, and an NSERC Undergraduate Student Research Award to K.J. A.Z. was supported by a Canadian Institutes of Health Research (CIHR) Strategic Training post-doctoral fellowship. Research at the Synchrotron Radiation Centre (SRC) is supported by NSF Award No. DMR-08442. Research performed at the Canadian Light Source (CLS) is supported by NSERC, the National Research Council, CIHR, the Canada Foundation for Innovation and the University of Saskatchewan. The technical assistance of Luca Quaroni and Tim May (CLS) and Robert Julian (SRC) is gratefully acknowledged.

## Authors' contribution

K.J. and A.S. contributed equally to this study.

## References

- Bartnicki-Garcia S (2002) Hyphal tip growth: outstanding questions. *Molecular Biology of Fungal Development* (Osiewacz HD, ed), pp. 29–58. Marcel Dekker, New York.
- Baldauf SL, Roger AJ, Wenk-Siefert I & Doolittle WF (2000) A kingdom-level phylogeny of eukaryotes based on combined protein data. *Science* **290**: 972–977.
- Beadle GW & Tatum EL (1941) Genetic control of biochemical reactions in *Neurospora*. *Proc Natl Acad Sci USA* **27**: 499–506.
- Becker ED & Farrar TC (1972) Fourier transform spectroscopy: new methods dramatically improve the sensitivity of infrared and nuclear magnetic resonance spectroscopy. *Science* **178**: 361–368.
- Blout ER & Fields M (1948) On the infrared spectra of nucleic acids and certain of their components. *Science* **107**: 252.
- Blout ER & Mellors RC (1949) Infrared spectra of tissues. *Science* **110**: 137–138.
- Chalmers JM & Griffiths PR (eds) (2002) *Handbook of Vibrational Spectroscopy: Theory and Instrumentation, Vol. 1–5*. John Wiley & Sons, Chichester.
- Coblentz WW (1911) Radiometric investigation of water of crystallization, light filters, and standard absorption bands. *Bull Natl Bur Stand (US)* **7**: 619–663.
- Darmon SE & Sutherland GBBM (1947) Infrared spectra and structure of natural and synthetic polypeptides. *J Am Chem Soc* **69**: 2074.
- d'Enfert C (1997) Fungal spore germination: insights from the molecular genetics of *Aspergillus nidulans* and *Neurospora crassa*. *Fung Genet Biol* **21**: 163–172.
- Dumas P, Jamin N, Teillaud JL, Miller LM & Beccard B (2004) Imaging capabilities of synchrotron infrared microspectroscopy. *Discuss Faraday Soc* **126**: 289–302.
- Elliott A & Ambrose EJ (1950) Structure of synthetic polypeptides. *Nature* **165**: 921–922.
- Everall NJ, Chalmers JM & Griffiths PR (eds) (2007) *Vibrational Spectroscopy of Polymers: Principles and Practice*. John Wiley & Sons, Chichester.
- Firon A & d'Enfert C (2002) Identifying essential genes in fungal pathogens of humans. *Trends Microbiol* **10**: 456–462.
- Fraser RDB (1950) Infra-red microspectrometry with a 0.8 N.A. reflecting microscope. *Discuss Faraday Soc* **9**: 378–383.
- Gallant M, Rak M, Szeghalmi A, Del Bigio MR, Westaway D, Yang J, Julian R & Gough KM (2006) Focally elevated creatine detected in amyloid precursor protein (APP) transgenic mice and Alzheimer disease brain tissue. *J Biol Chem* **281**: 5–8.
- Gough KM, Rak M, Bookatz A, Del Bigio M, Mai S & Westaway D (2005) Choices for tissue visualization with IR microspectroscopy. *Vib Spec* **38**: 133–141.
- Griffiths PR (1975) *Chemical Infrared Fourier Transform Spectroscopy*. Plenum, New York.
- Griffiths PR & De Haseth JA (1986) Chemical analysis. *Fourier Transform Infrared Spectrometry, Vol. 83*. John Wiley & Sons, New York.

- Holman H-YN, Martin MC & McKinney WR (2003) Tracking chemical changes in a live cell: biomedical applications of SR-FTIR spectromicroscopy. *Spectroscopy* **17**: 139–159.
- Howard RJ, Ferrari MA, Roach DH & Money NP (1991) Penetration of hard substrates by a fungus employing enormous turgor pressures. *Proc Natl Acad Sci USA* **88**: 11281–11284.
- Jamin N, Dumas P, Moncuit J, Fridman WH, Teillaud J-L, Carr GL & Williams GP (1998) Highly resolved chemical imaging of living cells by using synchrotron infrared microspectrometry. *Proc Nat Acad Sci USA* **95**: 4837–4840.
- Jilkinen K, Gough KM, Julian R & Kaminskyj SGW (2008) A sensitive method for examining whole cell biochemical composition in single cells of filamentous fungi using synchrotron FTIR spectromicroscopy. *J Inorg Biochem* **102**: 540–546.
- Kaminskyj SGW & Boire MR (2004) Ultrastructure of the *Aspergillus nidulans* *hypA1* restrictive phenotype shows defects in endomembrane arrays and polarized wall deposition. *Can J Bot* **82**: 807–814.
- Kaminskyj SGW & Dahms TES (2007) High spatial resolution surface imaging and analysis of fungal cells using SEM and AFM. *Micron* DOI: 10.1016/j.micron.2007.10.023.
- Karaffa L & Kubicek CP (2003) *Aspergillus niger* citric acid accumulation: do we understand this well working black box? *Appl Microbiol Biotechnol* **61**: 189–196.
- Márquez LM, Redman RS, Rodriguez RJ & Roossinck MJ (2007) A virus in a fungus in a plant – three-way symbiosis required for thermal tolerance. *Science* **315**: 513–515.
- Messerschmidt RG & Harthcock MA (eds) (1988) *Infrared Microspectroscopy: Theory and Applications. Practical Spectroscopy Series, Vol. 6*. Marcel Dekker, New York.
- Mie G (1908) Beiträge zur Optik trüber Medien, speziell kolloidaler Metallösungen. *Annal Physik* **33**: 377–455.
- Miller LM & Smith RL (2005) Synchrotrons versus globars, point-detectors versus focal plane arrays: selecting the best source and detector for specific infrared microspectroscopy and imaging applications. *Vib Spec* **38**: 237–240.
- Mohlenhoff B, Romeo M, Diem M & Wood BR (2005) Mie-type scattering and non Beer–Lambert absorption behaviour of human cells in infrared microspectroscopy. *Biophys J* **88**: 3635–3640.
- Montechiaro F, Hirschmugl CJ, Raven JA & Giordano M (2006) Homeostasis of cell composition during prolonged darkness. *Plant Cell Environ* **29**: 2198–2204.
- Naumann D (1985) The ultra rapid differentiation and identification of pathogenic bacteria using FT-IR and multivariate analysis. *Fourier and Computerized Spectroscopy* (Grasselli JG & Cameron DG, eds), pp. 268–269. Society of Photographic Instrumentation Engineers (SPIE) 553, Bellingham, WA.
- Navratil M, Mabbott GA & Arriaga EA (2006) Chemical microscopy applied to biological systems. *Analyt Chem* **78**: 4005–4017.
- Rak M (2007) Synchrotron infrared microspectroscopy of biological tissues: brain tissues from TgCRND8 Alzheimer's disease mice and developing scar tissue in rats. Ph.D. thesis, University of Manitoba.
- Szeghalmi A, Kaminskyj S & Gough KM (2007a) A synchrotron FTIR microspectroscopy investigation of fungal hyphae grown under optimal and stressed conditions. *Analyt Bioanalyt Chem* **387**: 1779–1789.
- Szeghalmi A, Kaminskyj S, Rösch P, Popp J & Gough KM (2007b) Time-fluctuations and imaging in the SERS spectra of fungal hypha grown on nanostructured substrates. *J Phys Chem B* **111**: 12916–12924.
- Toubas D, Essendoubi M, Adt I, Pinon JM, Manfait M & Sockalingum GD (2007) FTIR spectroscopy in medical mycology: applications to the differentiation and typing of *Candida*. *Analyt Bioanalyt Chem* **387**: 1729–1737.
- Wilson EB, Decius JC & Cross PC (1955) *Molecular Vibrations: the Theory of Infrared and Raman Vibrational Spectra*. McGraw-Hill, New York.